IC/96/246

INTERNATIONAL CENTRE FOR
THEORETICAL PHYSICS

THERMAL EXCITATIONS OF FRUSTRATED XY SPINS IN TWO DIMENSIONS

M. Benakli

H. Zheng

and

M. Gabay

MIRAMARE-TRIESTE

IC/96/246

United Nations Educational Scientific and Cultural Organization
and
International Atomic Energy Agency
INTERNATIONAL CENTRE FOR THEORETICAL PHYSICS

THERMAL EXCITATIONS OF FRUSTRATED XY SPINS IN TWO DIMENSIONS

M. Benakli
International Centre for Theoretical Physics, Trieste, Italy,

H. Zheng and M. Gabay
Laboratoire de Physique des Solides*, Université de Paris-Sud,
Bâtiment 510, 91405 Orsay Cedex, France.

MIRAMARE - TRIESTE
November 1996

*Laboratoire associé au CNRS.

ABSTRACT

We present a new variational approach to the study of phase transitions in frustrated 2D XY models. In the spirit of Villain's approach for the ferromagnetic case we divide thermal excitations into a low temperature long wavelength part (LW) and a high temperature short wavelength part (SW). In the present work we mainly deal with LW excitations and we explicitly consider the cases of the fully frustrated triangular (FFTXY) and square (FFSQXY) XY models. The novel aspect of our method is that it preserves the coupling between phase (spin angles) and chiral degrees of freedom. LW fluctuations consist of coupled phase and chiral excitations. As a result, we find that for frustrated systems the effective interactions between phase variables is long range and oscillatory in contrast to the unfrustrated problem. Using Monte Carlo (MC) simulations we show that our analytical calculations produce accurate results at all temperature T; this is seen at low T in the spin wave stiffness constant and in the staggered chirality; this is also the case near T_c: transitions are driven by the SW part associated with domain walls and vortices, but the coupling between phase and chiral variables is still relevant in the critical region. In that regime our analytical results yield the correct T dependence for bare couplings (given by the LW fluctuations) such as the Coulomb gas temperature T_{CG} of the frustrated XY models. In particular, we find that T_{CG} tracks chiral rather than phase fluctuations. Our results provide support for a single phase transition scenario in the FFTXY and FFSQXY models.

INTRODUCTION

Frustrated magnetic systems have been extensively studied, in part because they constitute non-disordered versions of spin-glasses[1,2]. They display rich low-temperature phases and remarkable phase transitions since frustration modifies the naive symmetry of the Hamiltonian. For spatial dimensions $D \geq 3$, Kawamura found by renormalization group (RG) techniques that frustrated $O(n)$ spin models belong to a new, "chiral" universality class[3]. For $D = 2$ and XY spins, which is our present concern, phase transitions are dominated by defects. Frustration results in additional chiral variables, which generate a discrete symmetry. In the fully frustrated case the Hamiltonian for a square lattice is believed to possess an $O(2) \times Z_2$ symmetry (see for instance Ref[4]); for the triangular lattice (FFTXY) one has the extra C_{3V} symmetry associated with the permutation of the three sublattices, thus adding the possibility of a Potts transition[5]. The transition associated with the $O(2)$ part (phases i.e. angular variables) would be Kosterlitz-Thouless (K-T)-like at a temperature T_{KT}[6] and the discrete Z_2 part (chiral variables) would be broken below a temperature T_{DS}. There is an ongoing controversy concerning the order in which these transitions should take place. RG calculations suggest that $T_C = T_{KT} = T_{DS}$ but two transitions are not ruled out[4,7–10] : in the single phase transition scenario, measurements of critical exponents for the chiral and of the central charge using MC and MC transfer matrix techniques[11] reveal non Ising behavior, providing support for Kawamura's claim of a new universality class even in 2D. This is also suggested by studies based on the selective breaking of certain symmetries[12–16]. Some MC studies performed on the FFTXY[17,5,15] and on the fully frustrated square (FFSQXY) models[12] yield a single phase transition; yet other MC simulations for the FFSQXY model and for the 1/2 integer Coulomb gas give two phase transitions very close in temperature[18–22].

In view of these unsettled issues the present paper has two objectives :

First we would like to give a quantitative description of the relevant excitations in FF systems. In doing so, we wish to assess the importance of the coupling between phase and chiral degrees of freedom at low temperature (T) and in the critical region. This would allow us to identify the nature of the critical fluctuations and to decide whether one should expect two phase transitions or just one.

Second we would like to test if the thermodynamic properties of the FFTXY and of the FFSQXY models are similar or not, and in particular if the nature of the phase transitions is different or the same for the two systems.

In order to get some insight into these issues we present a new analytical approach to study 2D XY frustrated systems. It is inspired by Villain's analysis for ferromagnetic (F) systems[23] where: (a) the partition and correlation functions are products of a Long Wavelength (LW) – spin waves – and of a Short Wavelength (SW) – vortex – contribution[24]; and (b) the long wavelength part is mapped *quantitatively* (by perturbation theory or variational scheme) onto the low temperature contribution of the original cosine Hamiltonian[25]. Steps (a) and (b) allow one to compute accurately all relevant thermodynamic quantities from $T = 0$ up to T_c. Our results are best summarized in the figures. In section I we begin with a brief discussion of steps (a) and (b) for the unfrustrated case and we show that a simple variational approach – the self-consistent harmonic approximation (SCHA)[25] – yields quantitative agreement with MC at all T so long as one considers thermodynamic variables sensitive to LW excitations (Fig (1)). Extending the method to FF systems produces incorrect results even at very low T (Fig (2)). Failure is due to the fact that a naive application of the variational approach eliminates chiral fluctuations. In section II we set up a new variational method (we call it NSCHA for new SCHA) which explicitly preserves the coupling between phase and chiral degrees of freedom. As a result, LW excitations consist of coupled spin waves (phase) and polar (chiral) fluctuations. This feature causes the effective interactions between phase variables to be long range and to oscillate in sign (Figs (3)-(4)). One may contrast this behavior with the unfrustrated case where phase couplings remain short range and positive in sign. Focusing on LW fluctuations, in section III we compare our results to MC simulations performed on the FFTXY and FFSQXY systems. For the FFTXY model we have done MC calculations for sizes up to 60×60, using $10^5 - 10^6$ MCS/spin and fluctuating boundary conditions[15,26]. For the FFSQXY lattice we have used available data from the literature : this is justified since we only use in a quantitative fashion data pertaining to LW excitations (i.e. results which are common to all studies). For all T MC simulations and analytical results agree closely: this is apparent in the LW contributions to the stiffness constant and to the chiral order parameter (Figs (5)-(8)). Above a characteristic temperature T^* defects become important and they ultimately drive the transition: we introduce a variable τ equ (36) which allows to track chiral domain walls. Fig (7) shows that they become relevant above T^*. Furthermore, Figs (5) and (6) show that for $T > T^*$ domains affect both the chiral order parameter and the spinwave stiffness constant. The relevance of the coupling between phase and chiral variables near the transitions is also visible in Fig (8) where we can see the agreement between analytical and MC predictions for the bare couplings

- here the Coulomb gas temperature T_{CG} (equ 37)-. Noteworthy is the fact that T_{CG} is connected to chiral variables in FF systems whereas it is a bare coupling constant for phase fluctuations in the unfrustrated situation (Fig (1)); this point is important in view of the fact that MC studies of FF systems assume that T_{CG} is a bare coupling for the *phase* variables (see discussion in section III). Our study thus suggests that the vanishing of the spinwave stiffness and of the chiral order parameter occur at the same T, for the FFTXY and for the FFSQXY models.

I. THE SELF CONSISTENT HARMONIC APPROXIMATION

A. The ferromagnetic case

Using standard notation the Hamiltonian reads

$$\mathcal{H} = - \sum_{<i,j>} J_{ij} cos(\theta_i - \theta_j) \qquad (1)$$

In the ferromagnetic case ($J_{ij} = J > 0$ for nearest neighbor pairs) Villain replaces the cosine potential by a parabolic form; $e^{\beta J cos(\theta_i - \theta_j)}$ is approximated by :

$$Const. \sum_{n_{ij}} e^{-\beta J_V (\theta_i - \theta_j - 2\pi n_{ij})^2} \qquad (2)$$

where the integers n_{ij} express the periodicity of the original interaction. The main features of the "Villain form " are that it includes both LW excitations (spin waves connected to the phases θ) and SW excitations (vortices connected to the lattice curl of the n) and that the partition function is the product of the LW and SW parts. Below T_{KT} the vortex part is essentially irrelevant (it simply introduces a dielectric constant $\epsilon_V \sim 1 + e^{-J/T}$) and LW properties are described by a harmonic spin wave hamiltonian with a spinwave stiffness constant $\gamma = J_V/\epsilon_V$. The importance of Villain's form stems from the fact that by applying the Migdal-Kadanoff scheme to the original cosine interaction, one iterates towards an effective harmonic spin wave theory below T_{KT}[24]. The shortcoming of (2) is that the coupling constant of the LW part is temperature independent whereas the original cosine form introduces interactions between spin waves. To deal with this issue one may use the self consistent harmonic approximation (SCHA)[25] : for the LW part one uses a variational hamiltonian

$$\mathcal{H}_0 = \frac{1}{2} \sum_{<i,j>} \tilde{J}_{ij} (\theta_i - \theta_j)^2 \qquad (3)$$

Anharmonicites of the cosine potential translate into a temperature dependence of $\tilde{J}_{ij}$.

The variational free energy is given by $F_{var} = F_0 + < \mathcal{H} - \mathcal{H}_0 >_{\mathcal{H}_0}$ (F_0 is the free energy for hamiltonian $\mathcal{H}_0$) and reads

$$F_{var} = -\frac{1}{2}\sum_{<i,j>} \tilde{J}_{ij} y_{ij} - \sum_{<i,j>} J_{ij} e^{-\frac{1}{2}y_{ij}} + \frac{T}{2}\log Det(\widetilde{\mathcal{J}}/T) \tag{4}$$

$\widetilde{\mathcal{J}}$ is the matrix with diagonal elements $\sum_k \tilde{J}_{ik}$ and off diagonal elements $-\tilde{J}_{ij}$. The quantities $y_{ij} =< (\theta_i - \theta_j)^2 >_{\mathcal{H}_0}$ are themselves functions of the variational parameters $\tilde{J}_{ij}$. Therefore, we may use y_{ij} as alternative variational parameters. The variational equations read :

$$\tilde{J}_{ij} = J_{ij} e^{-\frac{1}{2}y_{ij}} \tag{5}$$

with

$$y_{ij} = \frac{T}{2\pi^2}\iint_{BZ} d_2q \frac{(1 - cos\vec{q}.(\vec{r}_i - \vec{r}_j))}{\tilde{J}(0) - \tilde{J}(\vec{q})} \tag{6}$$

Here $\tilde{J}(\vec{q})$ is the Fourier transform of $\tilde{J}_{ij}$. In the ferromagnetic case, the effective interactions $\tilde{J}_{ij}$ only couple nearest neighbors. Their magnitude $\tilde{J}(T)$ is given by

$$\tilde{J}(T) = Je^{-\frac{J}{z\tilde{J}(T)}} \tag{7}$$

(z is the number of nearest neighbors of the lattice). One may then compute the spinwave stiffness matrix; its elements are given by the second derivatives of the free energy with respect to uniform twists of the phase[27]. For isotropic lattices the matrix is diagonal and all the elements are equal. In SCHA the constant is $\gamma_{SCHA} = \tilde{J}(T)$. We may then simply replace J_V in equ (2) above by γ_{SCHA}. Figs (1a) and (1b) show the temperature dependence of the SCHA stiffness for the square (SQ) and triangular (TR) lattices along with the MC result (denoted by $\gamma(T)$). At low T vortices contribute with a probability of order $e^{-zJ/T}$ so that SCHA and MC agree quite well. Near $T_{KT} \approx 0.892J$ (SQ lattice[28–30]) or $1.446J$ (TR lattice[31]) vortices cause a drop in $\gamma(T)$. Since SCHA only describes LW fluctuations it fails to produce a fall-off.

B. the Fully Frustrated case

The previous analysis is easily extended to the situation where spins are non collinear in equilibrium[32]. We rewrite the θ_i of equ (1) as:

$$\theta_i = \theta_i^0 + \varphi_i \tag{8}$$

where $\theta_i^0 =< \theta_i >_{\mathcal{H}_0}$ and the variational hamiltonian is

$$\mathcal{H}_0 = \frac{1}{2} \sum_{<i,j>} \tilde{J}_{ij} (\varphi_i - \varphi_j)^2 \tag{9}$$

In addition to the parameters $y_{ij} =< (\varphi_i - \varphi_j)^2 >_{\mathcal{H}_0}$ one has the extra variables θ_i^0. The variational equations now read

$$\tilde{J}_{ij} = J_{ij} cos(\theta_i^0 - \theta_j^0) . e^{-\frac{1}{2} y_{ij}} \tag{10}$$

$$\sum_{<i,j>} \tilde{J}_{ij} tan(\theta_i^0 - \theta_j^0) = 0 \tag{11}$$

and y_{ij} is given by equ(6). Denoting by $\vec{r}_i = (x_i, y_i)$ the vector connecting the origin of the lattice to site i and by $\vec{u}_{ij}$ the vector connecting nearest neighbor sites i and j, the solution θ_i^0 to these equations is independent of T and given by:

$$\theta_j^0 - \theta_i^0 \equiv \theta^0(\vec{r}_i + \vec{u}_{ij}) - \theta^0(\vec{r}_i) = A_{ij} + (-1)^{x_i + y_i} \alpha_{SQ} \; (mod\, 2\pi) \tag{12}$$

for the square lattice, along with the symmetry property

$$\theta^0(\vec{r}_i + \vec{u}_{ij}) - \theta^0(\vec{r}_i) = +(\theta^0(\vec{r}_i - \vec{u}_{ij}) - \theta^0(\vec{r}_i)) \tag{13}$$

and by:

$$\theta_j^0 - \theta_i^0 \equiv \theta^0(\vec{r}_i + \vec{u}_{ij}) - \theta^0(\vec{r}_i) = \vec{Q} . \vec{u}_{ij} = A_{ij} \pm \alpha_{TR} \; (mod\, 2\pi) \tag{14}$$

for the triangular lattice, along with the symmetry property

$$\theta^0(\vec{r}_i + \vec{u}_{ij}) - \theta^0(\vec{r}_i) = -(\theta^0(\vec{r}_i - \vec{u}_{ij}) - \theta^0(\vec{r}_i)) \tag{15}$$

Here $A_{ij} = -A_{ji} = \pi$ if $J_{ij} < 0$ and $A_{ij} = 0$ if $J_{ij} > 0$. α is a lattice dependent, temperature independent quantity. For the FFTXY lattice ($J_{ij} = -J < 0$) one has $\vec{Q} \propto (\frac{2\pi}{3}, \frac{2\pi}{\sqrt{3}})$ so that $\alpha_{TR} = \frac{\pi}{3}$. For the FFSQXY lattice - the so-called Villain odd model - ($J_{ij} = -J < 0$ every other row along, say, the horizontal direction and $J_{ij} = +J > 0$ otherwise) one finds $\alpha_{SQ} = \frac{\pi}{4}$. In addition $\tilde{J}_{ij}$ is a *nearest neighbor* interaction of magnitude

$$\tilde{J}(T) = J cos(\alpha) . e^{-\frac{T}{\tilde{J}(T)}} \tag{16}$$

Fig (2) shows the SCHA stiffnesses for the FFTXY lattice together with the MC result. Even at low T, $\tilde{J}(T)$ and $\gamma(T)$ differ significantly. The same effect is observed for the FFSQXY lattice. The reason for this discrepancy is clear : inserting equ (8) into equ (1) gives

$$\mathcal{H} = -\sum_{<i,j>} J_{ij}(cos(\theta_i^0 - \theta_j^0)cos(\varphi_i - \varphi_j) - sin(\theta_i^0 - \theta_j^0)sin(\varphi_i - \varphi_j)) \qquad (17)$$

Within SCHA the sin() term of equ (17) averages to zero. But this term precisely discriminates the $+\alpha$ solution from the $-\alpha$ solution in equs (12,14) and these two solutions correspond to the two chiral groundstates of the FF system. As a result SCHA washes out chiral fluctuations and maps the hamiltonian into an effective ferromagnetic phase problem since the J_{ij} are simply renormalized to $J_{ij}cos(\theta_i^0 - \theta_j^0)$.

Our analytical method was thus required to preserve the coupling between the two chiral states and to allow fluctuations of the chiralities. The next section shows that our approach then yields accurate results for the FF case. Furthermore, it also improves on the standard SCHA in the unfrustrated case.

II. NSCHA

Using equ (17) the partition function reads :

$$\mathcal{Z} = Tr_{\varphi_i} I_2(\varphi_i - \varphi_j) e^{\beta \sum_{<i,j>} J_{ij} cos(\theta_i^0 - \theta_j^0) cos(\varphi_i - \varphi_j)} \qquad (18)$$

where $I_2 = e^{-\beta \sum_{<i,j>} J_{ij} sin(\theta_i^0 - \theta_j^0) sin(\varphi_i - \varphi_j)}$. We rewrite I_2 as the sum of a term even in φ plus a term odd in φ :

$I_2(x) = \frac{1}{2}[I_2(x) + I_2(-x)] + \frac{1}{2}[I_2(x) - I_2(-x)]$

Now the trace over φ in equ (18) is constrained by equ (8) $\theta_i = \theta_i^0 + \varphi_i$ but for LW excitations we expect φ_i to fluctuate about 0, so that we can safely extend the domain of variation of φ_i to the interval $[-\pi, +\pi]$. As a result the odd term of I_2 drops out and the partition function reads

$\mathcal{Z} = Tr_{\varphi_i} e^{-\beta \mathcal{H}_{eff}}$ where

$$\begin{aligned} \mathcal{H}_{eff} = & -\sum_{<i,j>} J_{ij} cos(\theta_i^0 - \theta_j^0) cos(\varphi_i - \varphi_j) \\ & -T Log[cosh(\sum_{<i,j>} \beta J_{ij} sin(\theta_i^0 - \theta_j^0) sin(\varphi_i - \varphi_j))] \end{aligned} \qquad (19)$$

The second term on the r.h.s of equ (19) is the new relevant term. It has the following properties :

- it is a thermal contribution since it vanishes at $T = 0$
- it is zero for collinear systems (i.e. either unfrustrated or frustrated but with non chiral configurations)
- it couples chirality (θ_i^0 – more precisely $J_{ij}sin(\theta_i^0 - \theta_j^0)$ for each link (ij) equ (30) below –) and phase (φ_i) variables, allowing chiral fluctuations. Similarly, it preserves the symmetry between the two chiral groundstates.

We now compute the variational free energy associated with $\mathcal{H}_{eff}$ using the trial hamiltonian $\mathcal{H}_0$ (equ (9)). To do so we have to expand the $log(cosh)$ term of $\mathcal{H}_{eff}$ in power series of its argument. It is justified since the series amounts to a multipole expansion as is seen below. Besides, the leading term is the first term, especially at low T. $\mathcal{H}_{eff}$ then becomes

$$\begin{aligned}\mathcal{H}_{NSCHA} = & -\sum_{<i,j>} J_{ij}cos(\theta_i^0 - \theta_j^0)cos(\varphi_i - \varphi_j) \\ & -\frac{1}{2T}\sum_{<i,j>}\sum_{<k,l>} J_{ij}J_{kl}\, sin(\theta_i^0 - \theta_j^0)sin(\theta_k^0 - \theta_l^0) \\ & \qquad sin(\varphi_i - \varphi_j)sin(\varphi_k - \varphi_l)\end{aligned} \tag{20}$$

The variational equations for – what we call – the NSCHA (new SCHA) ensemble are:

$$\begin{aligned}\tilde{J}_{ij} = & J_{ij}\, cos(\theta_i^0 - \theta_j^0)\, e^{-\frac{1}{2}v_{ij}} \\ & +\frac{1}{2T}\sum_{k,l} J_{ij}J_{kl}\, sin(\theta_i^0 - \theta_j^0)sin(\theta_k^0 - \theta_l^0)e^{-\frac{1}{2}(v_{ij}+v_{kl}+v_{ik}+v_{jl}-v_{il}-v_{jk})} \\ & +\frac{1}{T}\sum_{k,l} J_{ik}J_{jl}\, sin(\theta_i^0 - \theta_k^0)sin(\theta_j^0 - \theta_l^0) \\ & \qquad cosh(y_{ij} + y_{kl} - y_{il} - y_{jk})\, e^{-\frac{1}{2}(v_{ik}+v_{jl})}\end{aligned} \tag{21}$$

$$\begin{aligned}& \sum_j J_{ij}\, sin(\theta_i^0 - \theta_j^0)\, e^{-\frac{1}{2}v_{ij}} \\ & -\frac{1}{2T}\sum_{j,k,l} J_{ij}J_{kl}\, cos(\theta_i^0 - \theta_j^0)sin(\theta_k^0 - \theta_l^0)e^{-\frac{1}{2}(v_{ij}+v_{kl}+v_{ik}+v_{jl}-v_{il}-v_{jk})} = 0\end{aligned} \tag{22}$$

Again $y_{ij} = < (\varphi_i - \varphi_j)^2 >_{\mathcal{H}_0}$ and

$$y_{ij} = \frac{T}{(2\pi^2)}\iint_{BZ} d_2q \frac{(1 - cos\vec{q}.(\vec{r}_i - \vec{r}_j))}{\tilde{J}(0) - \tilde{J}(\vec{q})} \tag{23}$$

For the FFTXY and FFTSQXY lattices it is easy to check that θ_i^0 is a temperature independent quantity and that its value is still given by equs (12,14)

Furthermore, equ (21) shows that $\tilde{J}_{ij}$ is no longer a short range interaction. In fact we find that for all T,

$$\tilde{J}_{ij} \sim \frac{1}{|\vec{r}_i - \vec{r}_j|^z} \tag{24}$$

for large distances $r = |\vec{r}_i - \vec{r}_j|$ (Fig (3)). This comes about because $y_{ij} \sim log(r)$ at large distances so that $y_{ik} + y_{jl} - y_{il} - y_{jk} \sim \frac{1}{r^2}$ in equ (21) : this contribution is quadrupolar like. Similarly, expanding the log(cosh) term to next order would produce a higher order multipolar contribution (see also Appendix A).

In addition, the sign of $\tilde{J}_{ij}$ varies with the relative orientation of i and j and, in the case of the FFSQXY lattice, with the distance between i and j Fig (4a) and (4b).

These features are to be contrasted with the results of SCHA yielding a positive nearest neighbor $\tilde{J}_{ij}$. The coupling between phase and chiral degrees of freedom has produced an oscillating, "long range" interaction between the phase variables. Because of these properties it is clear that renormalization group analyses (e.g. Migdal-Kadanoff) are not straighforward for FF systems.

Within NSCHA we can compute the phase stiffness constant. Owing to the isotropy of the lattices we have :

$$\Gamma(T) = \lim_{q_x \to 0} \frac{(\tilde{J}(0) - \tilde{J}(\vec{q}.\vec{u}_x))}{q_x^2} \tag{25}$$

where $\vec{u}_x$ is the unit vector along the horizontal direction of the lattice. Besides, within this new variational ensemble we also get a stiffness associated with the canting of the spins; considering a small variation of the nearest neighbor angle difference ${\theta_i}^0 - {\theta_j}^0$ from its equilibrium value in the form $\Delta\vec{u}_x.\vec{u}_{ij}$ we get:

$$\begin{aligned}
\gamma_{NSCHA}(T) &= \tfrac{\delta^2 F_{var}}{\delta(\Delta)^2}|_{\Delta \to 0} \\
&= \tfrac{1}{N}\Big(\textstyle\sum_{<i,j>} J_{ij}\, cos({\theta_i}^0 - {\theta_j}^0)(\vec{u}_{ij}.\vec{u}_x)^2 e^{-\frac{1}{2}v_{ij}} \\
&-\tfrac{1}{T}.\textstyle\sum_{<i,j>}\sum_{<k,l>} J_{ij}J_{kl}\,(\vec{u}_{ij}.\vec{u}_x)(\vec{u}_{kl}.\vec{u}_x)e^{-\frac{1}{2}(v_{ij}+v_{kl}+v_{ik}+v_{jl}-v_{il}-v_{jk})} \\
&\Big[cos({\theta_i}^0 - {\theta_j}^0)cos({\theta_k}^0 - {\theta_l}^0) + sin({\theta_i}^0 - {\theta_j}^0)sin({\theta_k}^0 - {\theta_l}^0)\Big]\Big)
\end{aligned} \tag{26}$$

It is easy to show that $\gamma_{NSCHA}(T)$ is nothing but the average of the exact spinwave stiffness $\gamma(T)$[5] in the ensemble $\mathcal{H}_0$, i.e.

$$\begin{aligned}
\gamma_{NSCHA}(T) = \tfrac{1}{N} &< \textstyle\sum_{<i,j>} J_{ij}\, cos(\theta_i - \theta_j)\,(\vec{u}_{ij}.\vec{u}_x)^2 \\
&-\tfrac{1}{T}\textstyle\sum_{<i,j>}\sum_{<k,l>} J_{ij}J_{kl}\,(\vec{u}_{ij}.\vec{u}_x)(\vec{u}_{kl}.\vec{u}_x)\,sin(\theta_i - \theta_j)sin(\theta_k - \theta_l) >_{\mathcal{H}_0}
\end{aligned} \tag{27}$$

A plot of $\Gamma(T)$ and $\gamma_{NSCHA}(T)$ versus T is shown for the TR lattice (Fig (5a)) and for the SQ lattice (Fig (5b)). We note that $\Gamma(T)$ and $\gamma_{NSCHA}(T)$ coincide at low T. This is explicitly demonstrated in Appendix B. In particular, we find that

$$\gamma_{NSCHA}(T) = \gamma_0(1 - \frac{T}{T_{c0}}) \tag{28}$$

- For the triangular lattice $\gamma_0 = \sqrt{3}/2J$ and $T_{c0} = \frac{1}{4/3 - \frac{3\sqrt{3}}{2\pi}} J \sim 1.975J$
- For the square lattice $\gamma_0 = \sqrt{2}/2J$ and $T_{c0} = \frac{1}{\frac{\sqrt{2}}{2} - \frac{\sqrt{2}}{2\pi}} J \sim 2.075J$

For both cases $T_{c0} \simeq 2J$ (Ref[33]).

Another quantity of interest is the staggered chirality

$$\sigma = \frac{1}{\mathcal{N}_P} \sum_P \frac{< \sum_{(k,l)\in P} \sigma_{kl} >_{\mathcal{H}_0}}{\sum_{(k,l)\in P} \sigma_{kl}(T=0)} \tag{29}$$

P denotes plaquettes of the same sublattices i.e. plaquettes in the same chiral state at $T = 0$. The summation $\sum_{(k,l)\in P}$ is performed over the links of plaquette P oriented clockwise. σ_{kl} is defined as :

$$\sigma_{kl} = J_{kl} sin(\theta_k - \theta_l) \tag{30}$$

(see below for a discussion on the definition of σ_{kl}).

Using equ (8), we have

$\sigma_{kl} = J_{kl}(cos({\theta_k}^0 - {\theta_l}^0) sin(\varphi_k - \varphi_l) + sin({\theta_k}^0 - {\theta_l}^0) cos(\varphi_k - \varphi_l))$

Within NSCHA the $sin(\varphi_k - \varphi_l)$ term drops out and $\sigma_{kl}(T=0) = J_{kl}(cos({\theta_k}^0 - {\theta_l}^0)$ so that

$$\sigma_{NSCHA} = e^{-\frac{1}{2}y_{kl}} \tag{31}$$

where k and l are *nearest neighbors* (y_{kl} has the same value for all the nearest neighbor sites l of any given site k). σ_{NSCHA} versus T is plotted in Fig (6) for the TR and SQ lattices.

To summarize the results of this section we see that LW thermal excitations in fully frustrated lattices are characterized by a strong coupling between chiral and phase degrees of freedom. The effective interaction between phase variables is long range and oscillatory – in contradistinction with the unfrustrated case –.

Let us now compare our results to those coming from Monte Carlo simulations.

III. MONTE CARLO VERSUS NSCHA

In order to test the predictions of NSCHA we used the results of Monte Carlo simulations. For the FFSQXY lattice we took data from the literature insofar as we did not seek to extract information about critical fluctuations. In that case there is agreement among the various studies. For the FFTXY and for the ferromagnetic triangular lattice recent data is rather scarce (Refs[17,5,15]) so that we performed our own simulations. We considered typical lattice sizes of 48×48 and ran $10^5 - 10^6$ MCS/spin. In order to minimize boundary effects we used fluctuating boundary conditions (Refs[15,26]). We monitored the following quantities :

- the spinwave stiffness constant $\gamma(T)$
- the staggered chirality σ equ (29):

several definitions of σ have been used in the literature. One of them is the definition we use here (see also Olsson[26]), others are[19]

$$\sigma^1 = \frac{1}{\mathcal{N}_P} < \sum_P Sign(\sum_{(k,l)\in P} \sigma_{kl}) > \tag{32}$$

where σ_{kl} is defined in equ (30) and $\mathcal{N}_P$ the number of plaquettes of each sublattice, or

$$\sigma' = \frac{1}{\mathcal{N}_P} < \sum_P \sum_{(k,l)\in P} \sigma'_{kl} > \tag{33}$$

with[21]

$$\sigma'_{kl} = \frac{1}{2\pi}(\theta_k - \theta_l - A_{kl}) \tag{34}$$

or with

$$\sigma'_{kl} = \frac{1}{2\pi}(\theta_k - \theta_l) \tag{35}$$

In equs (34,35) the angular determination of the terms in parenthesis is taken in the interval $]-\pi, +\pi]$. All these definitions lead to the same T dependence for σ in the critical region. For the square lattice this is reported by[19] for instance and for the triangular lattice this is seen in Fig (7) using the definitions equs (30) and (35).

- the chirality amplitude τ :

$$\tau = \frac{1}{\mathcal{N}_P} \sum_P \frac{< Abs(\sum_{(k,l)\in P} \sigma_{kl}) >}{Abs(\sum_{(k,l)\in P} \sigma_{kl}(T=0))} \tag{36}$$

using again the previous definitions for σ_{kl}. So long as chiralities are ordered on each sublattice τ and σ coincide. When domains of the "wrong" chiral state form on a given

sublattice the two quantities differ. Thus τ allows us to track the formation of domains and domain walls (where the chirality of a plaquette $\sum_{(k,l)\in P}\sigma_{kl}=0$). For the FFTXY lattice for instance Fig (7) shows that at T_c we have $\sim 30\%$ of positive chiralities, $\sim 30\%$ of negative chiralities and $\sim 40\%$ of a-chiral plaquettes on each sublattice.

• the Coulomb gas temperature T_{CG} :

This quantity monitors the bare (unrenormalized) coupling constant and allows to define the critical point for the XY model (Refs[34,30]). Within MC it is given by[30]

$$T_{CG}=\frac{T}{2\pi J_0},\quad J_0=J<cos(\theta_i-\theta_j)> \tag{37}$$

for nearest-neighbors i and j.

Figs (5a) and (5b) show $\Gamma(T),\gamma_{NSCHA}(T)$ and $\gamma(T)$ versus T. The three curves yield the same variation at low T. Furthermore, as could be expected from our previous discussion, $\gamma_{NSCHA}(T)$ tracks $\gamma(T)$ for $T\leq T^*$ ($T^*\sim 0.32J$ for the square lattice and $T^*\sim 0.35J$ for the triangular lattice); for $T>T^*$ the two curves move apart. Since NSCHA describes LW excitations but neglects SW excitations responsible for the transitions, this had to be expected.

Similarly, Fig (6) shows a comparison between NSCHA and MC for $\sigma(T)$; again the agreement is quite good for $T\leq T^*$. Moreover we also see from Fig (7) that T^* marks the temperature above which domain walls become important, since $\sigma(T)$ and $\tau(T)$ start to differ for $T\sim T^*$.

At this stage we might worry that the discrepancy between MC and NSCHA predictions for $T>T^*$ not only marks the point when defects become important but also signals the breakdown of the variational approach. In fact, NSCHA still yields accurate results for quantities sensitive to LW fluctuations including in the critical region. We see this by comparing the MC and the NSCHA J_0 entering the definition of the Coulomb gas temperature. T_{CG} represents the bare (unrenormalized) coupling constant when LW fluctuations are taken into account.

For instance, in the case of the square lattice, Olsson finds that $T_{CG}\sim 0.128$[22] at the KT transition ($T_{KT}\sim 0.446J$); this value is to be compared with the MC results by Grest[18] ($T_{CG}\sim 0.126$) and by Lee[20] ($T_{CG}\sim 0.1297$) on the half integer Coulomb gas representation of the FFSQXY.

Fig (8) shows $J_0(T)$ for the square and triangular lattices determined both in MC and in NSCHA. We notice that:

a) both determinations agree extremely well in the critical regime

b) J_0 *tracks the chiral variable couplings rather than the phase variable couplings* : Indeed, if we use for J_0 the definition given in equ (37) we find that in the NSCHA ensemble

$$J_{0NSCHA} = cos(\theta_i^0 - \theta_j^0)\sigma_{NSCHA} \tag{38}$$

and J_0 is therefore connected to the *chiral* variables. We have seen that the LW contribution to the chirality σ – given by equ (31) – does not vanish at the transition (σ becomes zero because of defects) so that J_{0NSCHA} is finite even in the critical regime. For instance, for the square lattice NSCHA gives $T_{CG} \sim 0.125$ using $T_{KT} = 0.446J$. By contrast, for the unfrustrated case, equ (37) gives $J_{0SCHA} = \tilde{J}(T)$ (see section I). So J_0 is connected to *phase* variables then (see also below).
In the frustrated case, if we replaced J_0 by $\Gamma(T)$ equ (25) we would find too high a value for T_{CG} (namely 0.139) compared to MC.

Similarly, for the triangular lattice MC gives $T_{KT} = 0.51J$ (Refs[5,15]) and $T_{CG} \sim 0.123$ to be compared with the NSCHA prediction (using equ (38)) $T_{CG} \sim 0.122$.

This result has direct implications for MC studies : these introduce a second critical temperature T_{DS} where chiral order vanishes. Some authors find $T_{KT} > T_{DS}$[19,9] whereas others predict $T_{KT} < T_{DS}$[18,21,22]. At T_{DS} critical exponents are found to be Ising-like by some authors[12,22] but non-Ising by others[19,21]. The magnitude of the jump of the spinwave stiffness constant or of the dielectric constant seen in MC appears universal for the FFTXY model ([33]) but non universal for the FFTSQXY model[33,18–21]. Recently, Olsson has argued that a correct analysis of the transitions in the case of the FFTSQXY requires extra care due to their closeness in temperature. As a result he finds a universal jump at T_{KT} and similarly Ising exponents at the chiral transition[22] in contradistinction with previous authors[33,18–21]. One should note that the claim of universality or non universality for the KT transition is based on a scaling a la Minnhagen for the magnitude of the jump : yet, according to Minnhagen's study this scaling should not hold (one might even expect a first order transition) given the value of the critical Coulomb gas temperature corresponding to T_{KT}[34,35].

Our results show that, because of the coupling between phase and chiral degrees of freedom, T_{CG} pertains to chiral variables; because of this coupling one might thus expect a single phase transition in these systems.

For the unfrustrated case – e.g. in the ferromagnetic limit –, equ (37) gives $J_{0SCHA} = \gamma_{SCHA} = \tilde{J}(T)$. Its temperature dependance compares reasonably well with MC (Fig

(1)). In fact MC and variational predictions agree extremely well if one compares J_0 to γ_{NSCHA}: NSCHA reduces to SCHA for the most part but even in the ferromagnetic case the stiffness $\gamma_{NSCHA}(T)$ equ (26) does not coincide with $\tilde{J}(T)$. Chiral fluctuations exist even when $\theta_i^0 = 0$. Equ (27) shows that $\gamma_{NSCHA}(T)$ represents the LW contribution to the stiffness constant γ, i.e. the bare coupling for the phase variables. So it is natural to identify $\frac{T}{2\pi\gamma_{NSCHA}}$ with T_{CG}. If we use $\gamma_{NSCHA}(T)$ in equ (37) we find analytically $T_{CG} = 0.198$ for the SQ lattice and $T_{CG} = 0.191$ for the TR lattice, to be compared with the MC values 0.1956 for the SQ lattice[30] and 0.192 for the TR lattice.

To summarize our results, we have constructed a variational ensemble (NSCHA) for fully frustrated XY systems in 2D. Testing its predictions with Monte Carlo simulations we see that our approach yields accurate results at all temperature – including in the critical regime – for quantities sensitive to long wavelength excitations. The key ingredient of the theory is the coupling between phase and chiral degrees of freedom and this coupling is always relevant. In particular, it causes the interaction between phase variables to be polar-like (long range and oscillatory). As a result, renormalization schemes assuming short range couplings might not be reliable.

If a Coulomb gas temperature is introduced it appears to track chiral variables rather than phase variables.

Monte Carlo simulations show that defects drive the transitions. In particular, chiral domains appear to affect the spinwave stiffness constant and chiralities in a similar fashion giving support for a single phase transition scenario.

The above results pertain to both the FFTXY and the FFSQXY lattices suggesting universality for fully frustrated systems.

For ferromagnetic systems NSCHA still improve on SCHA. The reason is because NSCHA incorporates fluctuations of the macroscopic phase (θ_0) about its equilibrium (zero) value, in contradistinction with SCHA. In that sense NSCHA is a canonical ensemble as opposed to SCHA which is a microcanonical ensemble. In that limit the Coulomb gas temperature is associated with the bare coupling constant of the phase variables.

ACKNOWLEDGMENTS

We enjoyed fruitful discussions on this problem with R. Eymard, E. Granato, M. Ney-Nifle and W.M. Saslow. Computer time on the Cray C98 was made possible by contract 960162 from IDRIS.

APPENDIX A:

In this appendix we show that in the limit of large distances $R = |\vec{r}_i - \vec{r}_j|$, $\tilde{J}_{ij}$ given by equ (21) behaves as $\tilde{J}_{ij} \sim \frac{1}{|\vec{r}_i - \vec{r}_j|^3}$ (equ (24)).

We start with the NSCHA variational equation for $\tilde{J}_{ij}$:

$$\begin{aligned}\tilde{J}_{ij} = & J_{ij}\cos(\theta_i^0 - \theta_j^0)e^{-\frac{1}{2}v_{ij}} \\ & + \frac{1}{2T}\sum_{k,l} J_{ij}J_{kl}\sin(\theta_i^0 - \theta_j^0)\sin(\theta_k^0 - \theta_l^0)e^{-\frac{1}{2}(v_{ij}+v_{kl}+v_{ik}+v_{jl}-v_{il}-v_{jk})} \\ & + \frac{1}{T}\sum_{k,l} J_{ik}J_{jl}\sin(\theta_i^0 - \theta_k^0)\sin(\theta_j^0 - \theta_l^0)\cosh(y_{ij}+y_{kl}-y_{il}-y_{jk})e^{-\frac{1}{2}(v_{ik}+v_{jl})}\end{aligned}$$

where $y_{ij} \equiv y(\vec{r}_j - \vec{r}_i)$ is given by equ (23) and where the angles $\{\theta_i^0\}$ satisfy equs (12, 14).

For the FFTXY the expression $J_{ij}\sin(\theta_j^0 - \theta_i^0)$ only depends upon $\vec{r}_j - \vec{r}_i$. For the FFSQXY lattice however, there are four different types of sites (see equ (12)) so that $J_{ij}\sin(\theta_j^0 - \theta_i^0)$ explicitly depends upon site i. Yet, for the FFSQXY lattice the quantity $(-1)^{x_i+y_i}J_{ij}\sin(\theta_j^0 - \theta_i^0)$ is independent of i .

Therefore, we introduce

$$\bar{J}_{\vec{r}_j - \vec{r}_i} = w^{x_i+y_i}J_{ij}\sin(\theta_j^0 - \theta_i^0), \tag{A1}$$

For the triangular lattice we choose $w = 1$ and for the square lattice we set $w = -1$. The quantity $\bar{J}$ defined in that way only depends upon $\vec{r}_j - \vec{r}_i$. $\bar{J}$ possesses the following symmetry properties :

$$\bar{J}(-\vec{\epsilon}) = -\bar{J}(\vec{\epsilon}) \tag{A2}$$

for the TR lattice and

$$\bar{J}(-\vec{\epsilon}) = \bar{J}(\vec{\epsilon}), \qquad \bar{J}(\vec{u_x}) = -\bar{J}(\vec{u_y}) \tag{A3}$$

for the SQ lattice.

In the following we introduce the notations $\vec{R} = \vec{r}_j - \vec{r}_i$, $\vec{\epsilon}' = \vec{r}_l - \vec{r}_j$, $\vec{\epsilon} = \vec{r}_k - \vec{r}_i$. For large R, only the third term in the r.h.s. of equ (21) contributes, since J_{ij} is a nearest neighbor interaction. Using the fact that $\bar{J}_{ij}$ is independent of i, that we have the symmetry properties, equs (A2,A3) and that the value of y_{ij} is the same for all the *nearest neighbors* j of a given site i (by symmetry) we get

$$\tilde{J}_{\vec{R}} = -\frac{1}{T}e^{-y(\vec{\epsilon}_0)}w^{R_x+R_y}\sum_{\vec{\epsilon},\vec{\epsilon}'}\bar{J}_{\vec{\epsilon}}\bar{J}_{\vec{\epsilon}'}\cosh\frac{1}{2}(y(\vec{R}+\vec{\epsilon}+\vec{\epsilon}')+y(\vec{R})-y(\vec{R}+\vec{\epsilon})-y(\vec{R}+\vec{\epsilon}'))$$

where $\vec{\epsilon_0}$ is any nearest neighbor vector connecting two sites.

We denote by $\Delta y(\vec{R},\vec{\epsilon},\vec{\epsilon'})$ the following quantity:

$\Delta y(\vec{R},\vec{\epsilon},\vec{\epsilon'}) \equiv y(\vec{R}+\vec{\epsilon}+\vec{\epsilon'}) + y(\vec{R}) - y(\vec{R}+\vec{\epsilon}) - y(\vec{R}+\vec{\epsilon'})$. In the large R limit we expand y in powers of R; with :

$$\Delta_2 y(\vec{R},\vec{\epsilon},\vec{\epsilon'}) \equiv -\frac{1}{2}\sum_{\alpha,\beta}(\epsilon'_\alpha\epsilon_\beta + \epsilon_\alpha\epsilon'_\beta)\frac{\partial^2 y(\vec{R})}{\partial R_\alpha \partial R_\beta}$$

and

$$\Delta_3 y(\vec{R},\vec{\epsilon},\vec{\epsilon'}) \equiv \frac{1}{6}\sum_{\alpha,\beta,\gamma}(-\epsilon'_\alpha\epsilon'_\beta\epsilon_\gamma - \epsilon'_\alpha\epsilon_\gamma\epsilon'_\beta - \epsilon'_\beta\epsilon'_\gamma\epsilon_\alpha + \epsilon_\alpha\epsilon_\beta\epsilon'_\gamma + \epsilon_\alpha\epsilon_\gamma\epsilon'_\beta + \epsilon_\beta\epsilon_\gamma\epsilon'_\alpha)\frac{\partial^3 y(\vec{R})}{\partial R_\alpha \partial R_\beta \partial R_\gamma}$$

we have that $\Delta y(\vec{R},\vec{\epsilon},\vec{\epsilon'}) = \Delta_2 y(\vec{R},\vec{\epsilon},\vec{\epsilon'}) + \Delta_3 y(\vec{R},\vec{\epsilon},\vec{\epsilon'}) + \cdots$

In Appendix B we show that $\tilde{J}_0 - \tilde{J}_{\vec{q}} \sim \Gamma q^2$ for small $\vec{q}$ so that - using equ (23) - we get $y(\vec{R}) \sim \log|\vec{R}|$ for large R. As a result

$$\frac{\partial^2 y(\vec{R})}{\partial R_\alpha \partial R_\beta} \sim \frac{1}{R^2}, \qquad \frac{\partial^3 y(\vec{R})}{\partial R_\alpha \partial R_\beta \partial R_\gamma} \sim \frac{1}{R^3} \tag{A4}$$

Expanding cosh() we get:

$$\tilde{J}_{\vec{R}} = -\frac{1}{T}e^{-y(\vec{\epsilon_0})}w^{R_x+R_y}\sum_{\vec{\epsilon'},\vec{\epsilon}}\bar{J}_{\vec{\epsilon}}\bar{J}_{\vec{\epsilon'}}\{1 + \frac{1}{2}[\frac{1}{2}\Delta y(\vec{R},\vec{\epsilon},\vec{\epsilon'})]^2 + \cdots\} \tag{A5}$$

that is

$$\begin{aligned}\tilde{J}_{\vec{R}} = -\frac{1}{T}e^{-y(\vec{\epsilon_0})}w^{R_x+R_y}\sum_{\vec{\epsilon'},\vec{\epsilon}}\bar{J}_{\vec{\epsilon}}\bar{J}_{\vec{\epsilon'}}\{1 + \frac{1}{8}[\Delta_2 y(\vec{R},\vec{\epsilon},\vec{\epsilon'})]^2 \\ + \frac{1}{4}[\Delta_2 y(\vec{R},\vec{\epsilon},\vec{\epsilon'})][\Delta_3 y(\vec{R},\vec{\epsilon},\vec{\epsilon'})] + \frac{1}{8}[\Delta_3 y(\vec{R},\vec{\epsilon},\vec{\epsilon'})]^2\} + O(R^{-7})\end{aligned} \tag{A6}$$

- for the triangular lattice, using equ (A2) we have

$\sum_{\vec{\epsilon'},\vec{\epsilon}}\bar{J}_{\vec{\epsilon}}\bar{J}_{\vec{\epsilon'}} = 0,$

$\sum_{\vec{\epsilon'},\vec{\epsilon}}\bar{J}_{\vec{\epsilon}}\bar{J}_{\vec{\epsilon'}}\left[\Delta_2 y(\vec{R},\vec{\epsilon},\vec{\epsilon'})\right]^2 = 0,$

$\sum_{\vec{\epsilon'},\vec{\epsilon}}\bar{J}_{\vec{\epsilon}}\bar{J}_{\vec{\epsilon'}}[\Delta_2 y(\vec{R},\vec{\epsilon},\vec{\epsilon'})][\Delta_3 y(\vec{R},\vec{\epsilon},\vec{\epsilon'})] = 0.$

so that

$$\tilde{J}_{\vec{R}} \simeq -\frac{1}{T}e^{-y(\vec{\epsilon_0})}\sum_{\vec{\epsilon'},\vec{\epsilon}}\bar{J}_{\vec{\epsilon}}\bar{J}_{\vec{\epsilon'}}\frac{1}{8}[\Delta_3 y(\vec{R},\vec{\epsilon},\vec{\epsilon'})]^2 \sim \frac{1}{R^6} \tag{A7}$$

- for the square lattice, using equ (A3) we have

$\sum_{\vec{\epsilon'},\vec{\epsilon}}\bar{J}_{\vec{\epsilon}}\bar{J}_{\vec{\epsilon'}} = 0,$

but $\sum_{\vec{\epsilon}',\vec{\epsilon}} \bar{J}_{\vec{\epsilon}} \bar{J}_{\vec{\epsilon}'} [\Delta_2 y(\vec{R},\vec{\epsilon},\vec{\epsilon}')]^2 \neq 0.$

so that

$$\tilde{J}_{\vec{R}} \simeq -\frac{1}{T} e^{-v(\vec{\epsilon}_0)} (-1)^{R_x+R_y} \sum_{\vec{\epsilon}',\vec{\epsilon}} \bar{J}_{\vec{\epsilon}} \bar{J}_{\vec{\epsilon}'} \frac{1}{8} [\Delta_2 y(\vec{R},\vec{\epsilon},\vec{\epsilon}')]^2 \sim \frac{1}{R^4} \tag{A8}$$

We note the sign alternation due to the $(-1)^{R_x+R_y}$ term for the FFSQXY lattice (see Fig. 4) .

APPENDIX B:

In this appendix we compute $\gamma_{NSCHA}(T)$ (equ (26)) and $\Gamma(T)$ (equ (25)), at low T. We show that for the FFTXY and FFSQXY lattices $\gamma_{NSCHA}(T) - \Gamma(T) = O(T^2)$.

We start with equ (21). Using the same notations as in Appendix A we have

$$\begin{aligned}\tilde{J}(\vec{R}) = & |J_{\vec{R}}| \cos\alpha(\vec{R}) e^{-\frac{1}{2}v(\vec{R})} \\ & -\frac{1}{4T}\sum_{\vec{r}}\sum_{\vec{\varepsilon},\vec{\varepsilon}'} w^{r_x+r_y} \bar{J}_{\vec{\varepsilon}}\bar{J}_{\vec{\varepsilon}'} e^{-\frac{1}{2}(v(\vec{\varepsilon})+v(\vec{\varepsilon}')+v(\vec{r}+\vec{\varepsilon}+\vec{\varepsilon}')+v(\vec{r})-v(\vec{r}+\vec{\varepsilon})-v(\vec{r}+\vec{\varepsilon}'))} \\ & \times(\delta(\vec{R}-\vec{\varepsilon}) + \delta(\vec{R}-\vec{\varepsilon}') + \delta(\vec{R}-\vec{r}) + \delta(\vec{R}-(\vec{r}+\vec{\varepsilon}+\vec{\varepsilon}')) \\ & -\delta(\vec{R}-\vec{\varepsilon}-\vec{r}) - \delta(\vec{R}-\vec{\varepsilon}'-\vec{r}))\end{aligned} \tag{B1}$$

where $\delta(...)$ denotes the Kronecker delta symbol, where $\alpha(\vec{R})$ was defined in equs (12,14) and where the expression is written in such a way as to preserve the symmetry under the transformation $\varepsilon \leftrightarrow \varepsilon'$.

We now Fourier transform equ (B1) :

$$\begin{aligned}\tilde{J}_{\vec{q}} = & \sum_{\vec{R}} |J_{\vec{R}}| \cos\alpha(\vec{R}) e^{-\frac{1}{2}v(\vec{R})} e^{-i\vec{q}.\vec{R}} \\ & -\frac{1}{4T}\sum_{\vec{R}}\sum_{\vec{r}}\sum_{\vec{\varepsilon},\vec{\varepsilon}'} w^{r_x+r_y} \bar{J}_{\vec{\varepsilon}}\bar{J}_{\vec{\varepsilon}'} e^{-\frac{1}{2}(v(\vec{\varepsilon})+v(\vec{\varepsilon}')+v(\vec{r}+\vec{\varepsilon}+\vec{\varepsilon}')+v(\vec{r})-v(\vec{r}+\vec{\varepsilon})-v(\vec{r}+\vec{\varepsilon}'))} \\ & \times(\delta(\vec{R}-\vec{\varepsilon}) + \delta(\vec{R}-\vec{\varepsilon}') + \delta(\vec{R}-\vec{r}) + \delta(\vec{R}-(\vec{r}+\vec{\varepsilon}+\vec{\varepsilon}')) \\ & -\delta(\vec{R}-\vec{\varepsilon}-\vec{r}) - \delta(\vec{R}-\vec{\varepsilon}'-\vec{r}))e^{-i\vec{q}.\vec{R}}\end{aligned} \tag{B2}$$

setting

$$\begin{aligned}B \equiv & \sum_{\vec{R}}(\delta(\vec{R}-\vec{\varepsilon}) + \delta(\vec{R}-\vec{\varepsilon}') + \delta(\vec{R}-\vec{r}) + \delta(\vec{R}-(\vec{r}+\vec{\varepsilon}+\vec{\varepsilon}')) \\ & -\delta(\vec{R}-\vec{\varepsilon}-\vec{r}) - \delta(\vec{R}-\vec{\varepsilon}'-\vec{r}))e^{-i\vec{q}.\vec{R}}\end{aligned}$$

we see that $B = e^{-i\vec{q}.\vec{\varepsilon}} + e^{-i\vec{q}.\vec{\varepsilon}'} + e^{-i\vec{q}.\vec{r}} + e^{-i\vec{q}.(\vec{r}+\vec{\varepsilon}+\vec{\varepsilon}')} - e^{-i\vec{q}.(\vec{r}+\vec{\varepsilon})} - e^{-i\vec{q}.(\vec{r}+\vec{\varepsilon}')}$

Since we wish to compute

$$\Gamma(T) = \lim_{q_x\to 0}\frac{1}{q_x^2}(\tilde{J}(0) - \tilde{J}_{\vec{q}.\vec{u}_x}) \tag{B3}$$

we may expand B to second order in q:

$B = 2 - (\vec{q}.\vec{\varepsilon})(\vec{q}.\vec{\varepsilon}') + O(q^3)$

and thus :

$$\Gamma(T) = \frac{1}{2}\sum_{\vec{\epsilon}} |J_{\vec{\epsilon}}| \cos\alpha(\vec{\epsilon})(\vec{u_x}.\vec{\epsilon})^2 e^{-\frac{1}{2}v(\vec{\epsilon})} \tag{B4}$$
$$+\frac{1}{4T}\sum_{\vec{r}}\sum_{\vec{\epsilon},\vec{\epsilon'}} w^{r_x+r_y} \bar{J}_{\vec{\epsilon}}\bar{J}_{\vec{\epsilon'}}(\vec{u_x}.\vec{\epsilon})(\vec{u_x}.\vec{\epsilon'})$$
$$\times e^{-\frac{1}{2}(v(\vec{\epsilon})+v(\vec{\epsilon'})+v(\vec{r}+\vec{\epsilon}+\vec{\epsilon'})+v(\vec{r})-v(\vec{r}+\vec{\epsilon})-v(\vec{r}+\vec{\epsilon'}))}$$

Similarly, $\gamma_{NSCHA}(T)$ equ (26) is given by

$$\gamma_{NSCHA}(T) = \frac{1}{2}\sum_{\vec{\epsilon}} |J_{\vec{\epsilon}}| \cos\alpha(\vec{\epsilon})(\vec{\epsilon}.\vec{u_x})^2 e^{-\frac{1}{2}v(\vec{\epsilon})} \tag{B5}$$
$$-\frac{1}{4T}\sum_{\vec{r}}\sum_{\vec{\epsilon},\vec{\epsilon'}}(\vec{\epsilon}.\vec{u_x})(\vec{\epsilon'}.\vec{u_x})(|J_{\vec{\epsilon}}|\cos\alpha(\vec{\epsilon})|J_{\vec{\epsilon'}}|\cos\alpha(\vec{\epsilon'}) - w^{r_x+r_y}\bar{J}_{\vec{\epsilon}}\bar{J}_{\vec{\epsilon'}})$$
$$\times e^{-\frac{1}{2}(v(\vec{\epsilon})+v(\vec{\epsilon'})+v(\vec{r}+\vec{\epsilon}+\vec{\epsilon'})+v(\vec{r})-v(\vec{r}+\vec{\epsilon})-v(\vec{r}+\vec{\epsilon'}))}$$

We see that the difference between the expression of $\Gamma(T)$ and the expression of $\gamma_{NSCHA}(T)$ comes from the term proportional to $\cos\alpha(\vec{\epsilon})\cos\alpha(\vec{\epsilon'})$.

With the notations:

$$A = \frac{1}{2}\sum_{\vec{\epsilon}} |J_{\vec{\epsilon}}| \cos(\alpha(\vec{\epsilon}))(\vec{u}_x\vec{\epsilon})^2 e^{-\frac{1}{2}v(\vec{\epsilon})}$$

$$S = \frac{1}{4}\sum_{\vec{r}}\sum_{\vec{\epsilon},\vec{\epsilon'}} w^{r_x+r_y}\bar{J}_{\vec{\epsilon}}\bar{J}_{\vec{\epsilon'}}(\vec{u}_x.\vec{\epsilon})(\vec{u}_x.\vec{\epsilon'})$$
$$\times e^{-\frac{1}{2}(v(\vec{\epsilon})+v(\vec{\epsilon'})+v(\vec{r}+\vec{\epsilon}+\vec{\epsilon'})+v(\vec{r})-v(\vec{r}+\vec{\epsilon})-v(\vec{r}+\vec{\epsilon'}))}$$

$$C = \frac{1}{4}\sum_{\vec{r}}\sum_{\vec{\epsilon},\vec{\epsilon'}} |J_{\vec{\epsilon}}| \cos(\alpha(\vec{\epsilon}))|J_{\vec{\epsilon'}}| \cos(\alpha(\vec{\epsilon'}))(\vec{u}_x.\vec{\epsilon})(\vec{u}_x.\vec{\epsilon'})$$
$$\times e^{-\frac{1}{2}(v(\vec{\epsilon})+v(\vec{\epsilon'})+v(\vec{r}+\vec{\epsilon}+\vec{\epsilon'})+v(\vec{r})-v(\vec{r}+\vec{\epsilon})-v(\vec{r}+\vec{\epsilon'}))}$$

$\gamma_{NSCHA}(T)$ and $\Gamma(T)$ read :

$$\gamma_{NSCHA}(T) = A - \frac{1}{T}C + \frac{1}{T}S$$
$$\Gamma(T) = A + \frac{1}{T}S$$

Expanding A, C and S in T yields:

$C = C^0 + C^1T + C^2T^2 + O(T^3)$ and $S = S^0 + S^1T + S^2T^2 + O(T^3)$

We set $g(\vec{r}) \equiv v(\vec{r})/T$ such that $g(\vec{r})$ approaches a finite limit as $T \to 0$.

<u>to order T^0 :</u>

$$C^0 = \frac{1}{4}\sum_{\vec{r}}\sum_{\vec{\epsilon},\vec{\epsilon'}} |J_{\vec{\epsilon}}| \cos\alpha(\vec{\epsilon})|J_{\vec{\epsilon'}}| \cos\alpha(\vec{\epsilon'})(\vec{\epsilon}.\vec{u}_x)(\vec{\epsilon'}.\vec{u}_x) = 0$$

$$S^0 = -\frac{1}{4}\sum_{\vec{r}}\sum_{\vec{\epsilon},\vec{\epsilon'}} w^{r_x+r_y}\bar{J}_{\vec{\epsilon}}\bar{J}_{\vec{\epsilon'}}(\vec{\epsilon}.\vec{u}_x)(\vec{\epsilon'}.\vec{u}_x) = 0$$

C^0 is clearly zero when one sums over $\vec{\epsilon}$ and $\vec{\epsilon}'$

$S^0 = 0$ for the SQ lattice because $w = -1$ so that $\sum_{\vec{r}} w^{r_x+r_y} = 0$; $S^0 = 0$ for the TR lattice because $\sum_{\vec{\epsilon}} \bar{J}_{\vec{\epsilon}}(\vec{\epsilon}.\vec{u}_x) = 0$

to order T^1 :

$$C^1 = \frac{1}{4}\sum_{\vec{r}}\sum_{\vec{\epsilon},\vec{\epsilon}'} |J_{\vec{\epsilon}}| \cos\alpha(\vec{\epsilon})|J_{\vec{\epsilon}}| \cos\alpha(\vec{\epsilon})(\vec{\epsilon}.\vec{u}_x)(\vec{\epsilon}'.\vec{u}_x)$$
$$\cdot\frac{1}{2}(g(\vec{\epsilon}) + g(\vec{\epsilon}') + g(\vec{r}+\vec{\epsilon}+\vec{\epsilon}') + g(\vec{r}) - g(\vec{r}+\vec{\epsilon}) - g(\vec{r}+\vec{\epsilon}')))$$
$$= 0$$

$$S^1 = \frac{1}{4}\sum_{\vec{r}}\sum_{\vec{\epsilon},\vec{\epsilon}'} w^{r_x+r_y} \bar{J}_{\vec{\epsilon}}\bar{J}_{\vec{\epsilon}'}(\vec{\epsilon}.\vec{u}_x)(\vec{\epsilon}'.\vec{u}_x)$$
$$(-\frac{1}{2})(g(\vec{\epsilon}) + g(\vec{\epsilon}') + g(\vec{r}+\vec{\epsilon}+\vec{\epsilon}') + g(\vec{r}) - g(\vec{r}+\vec{\epsilon}) - g(\vec{r}+\vec{\epsilon}'))$$
$$= 0$$

Both C^1 and S^1 equal zero, owing to the parity in $\vec{\epsilon}$ and $\vec{\epsilon}'$, and using the fact that $\sum_{\vec{r}} g(\vec{r}+\vec{a}) = \sum_{\vec{r}} g(\vec{r})$ whenever $\vec{a}$ is any vector connecting sites of the lattice.

to order T^2 :

$$C^2 = \frac{1}{4}\sum_{\vec{r}}\sum_{\vec{\epsilon},\vec{\epsilon}'} |J_{\vec{\epsilon}}| \cos\alpha(\vec{\epsilon})|J_{\vec{\epsilon}'}| \cos\alpha(\vec{\epsilon}')(\vec{\epsilon}.\vec{u}_x)(\vec{\epsilon}'.\vec{u}_x)$$
$$\cdot\frac{1}{8}(g(\vec{\epsilon}) + g(\vec{\epsilon}') + g(\vec{r}+\vec{\epsilon}+\vec{\epsilon}') + g(\vec{r}) - g(\vec{r}+\vec{\epsilon}) - g(\vec{r}+\vec{\epsilon}'))^2$$

$$S^2 = \frac{1}{4}\sum_{\vec{r}}\sum_{\vec{\epsilon},\vec{\epsilon}'} w^{r_x+r_y} \bar{J}_{\vec{\epsilon}}\bar{J}_{\vec{\epsilon}'}$$
$$\cdot\frac{1}{8}(g(\vec{\epsilon}) + g(\vec{\epsilon}') + g(\vec{r}+\vec{\epsilon}+\vec{\epsilon}') + g(\vec{r}) - g(\vec{r}+\vec{\epsilon}) - g(\vec{r}+\vec{\epsilon}'))^2$$

Using the same properties as for the terms of order T we find:

$$C^2 = 0$$
$$S^2 = \frac{1}{4}\sum_{\vec{r}}\sum_{\vec{\epsilon},\vec{\epsilon}'} w^{r_x+r_y} \bar{J}_{\vec{\epsilon}}\bar{J}_{\vec{\epsilon}'}$$
$$\cdot\frac{1}{2}g(\vec{r})g(\vec{r}+\vec{\epsilon}+\vec{\epsilon}')$$

Also expanding A to order T gives :

$$A = \frac{1}{2}\sum_{\vec{\epsilon}} |J_{\vec{\epsilon}}| \cos\alpha(\vec{\epsilon}).(\vec{u}_x\vec{\epsilon})^2(1 - \frac{T}{2}g(\vec{\epsilon})) + O(T^2)$$

From these calculations we deduce that $\gamma_{NSCHA}(T) = \Gamma(T)$ to order T ($C = O(T^3)$). At this order we may simply replace $\tilde{J}_{\vec{q}}$ by $J_{\vec{q}}$ in the expression of $g(\vec{r})$ and we find that (equ (28))

$$\gamma_{NSCHA}(T) = \gamma_0(1 - \frac{T}{T_{c0}}) \tag{B6}$$

with

- For the triangular lattice $\gamma_0 = \sqrt{3}/2J$ and $T_{c0} = \frac{1}{4/3 - \frac{3\sqrt{3}}{2\pi}} J \sim 1.975J$
- For the square lattice $\gamma_0 = \sqrt{2}/2J$ and $T_{c0} = \frac{1}{\frac{\sqrt{2}}{2} - \frac{\sqrt{2}}{2\pi}} J \sim 2.075J$

REFERENCES

[1] J. Villain J. Phys. **C10**, 4793 (1977); J. Phys. (Paris) **38**, 26 (1977); **C11**, 745 (1978)

[2] H.T. Diep, Magnetic Systems with competing interactions, World Scientific, (1994)

[3] H. Kawamura, Phys. Rev. **B38**, 4916 (1988); H. Kawamura, J. Phys. Soc. Jpn. **61**, 1299 (1992)

[4] M Yosefin and E. Domany, Phys. Rev. **B32**, 1778 (1985)

[5] D.H. Lee, J.D. Joanopoulos, J.W. Negele, and D.P. Landau, Phys. Rev. **B33**, 450 (1986)

[6] J.M. Kosterlitz, D.J. Thouless, J. Phys. **C6**, 1181 (1973)

[7] E. Granato, J.M. Kosterlitz and J. Poulter, Phys. Rev. **B33**, 4767 (1986)

[8] J. Lee, J.M. Kosterlitz, and E. Granato, Phys. Rev. **B43**, 11531 (1991)

[9] J-R Lee and S. Teitel, Phys. Rev. **B46**, 3247 (1992)

[10] S.E. Korshunov, J. Stat. Phys. **43**, 17 (1986)

[11] M.P Nightingale, E. Granato, J.M. Kosterlitz, Phys. Rev **B52**,7402 (1995)

[12] B. Berge, H.T. Diep, A. Ghazali, and P. Lallemand, Phys. Rev. **B34**, 3177 (1986)

[13] M. Gabay, T. Garel, G. Parker and W.M. Saslow, Phys. Rev. **B40** 264 (1989)

[14] H. Eikmans and J.E. van Himbergen, H.J.F. Knops and J.M. Thjissen, Phys. Rev. **B39**, 11759 (1989)

[15] W.M. Saslow, M. Gabay and W.-M. Zhang, Phys. Rev. Lett **68**, 3627 (1992)

[16] W.-M. Zhang, W.M. Saslow, M. Gabay and M. Benakli , Phys. Rev. **B48**, 10204 (1993)

[17] W.Y. Shih and D. Stroud, Phys. Rev. **B30**, 6774 (1984)

[18] G. Grest, Phys. Rev. **B39**, 9267 (1989)

[19] G. Ramirez-Santiago, J.V. José, Phys. Rev. **B49**, 9567 (1994)

[20] J-R Lee, Phys. Rev. **B49**, 3317 (1994)

[21] S. Lee and K-C Lee, Phys. Rev. **B49**, 15184 (1994)

[22] P. Olsson, Phys.Rev. Lett. **75**, 2758 (1995)

[23] J. Villain, J. Phys. (Paris) **36**, 581 (1975)

[24] J.V. José, L.P. Kadanoff, S. Kirkpatrick, D.R. Nelson, Phys. Rev. **B16**, 1217 (1977)

[25] V.L. Pokrovskii and G.V. Uimin, Phys. Lett. **A45**, 467 (1973); J. Villain, J. Phys. (Paris), **35**, 27 (1974); Y.E. Lozovik and S.G. Akapov, J. Phys **C14**, L31 (1981)

[26] P. Olsson, Phys. Rev. **B52**, 4511 (1995)

[27] T. Ohta and D. Jasnow, Phys. Rev. **B20**, 139 (1979)

[28] H. Weber and P. Minnhagen, Phys. Rev. **B37**, 5986 (1988)

[29] N. Schultka and E. Manousakis, Phys. Rev. **B49**, 12071 (1994)

[30] P. Olsson, Phys. Rev. **B52**, 4526 (1995)

[31] P. Butera and M. Comi, Phys. Rev. **B50**, 3052 (1994)

[32] D. Ariosa, A. Vallat, H. Beck, J. de Physique **51**, 1373 (1990)

[33] P. Minnhagen, Phys. Rev. **B32**, 7548 (1985)

[34] P. Minnhagen, Rev. Mod. Phys. **59**, 1001 (1987)

[35] P. Minnhagen and M. Wallin, Phys. Rev. **B40**, 5109 (1989); A. Jonsson, P. Minnhagen and M. Nylen, Phys.Rev. Lett. **70**, 1327 (1993)

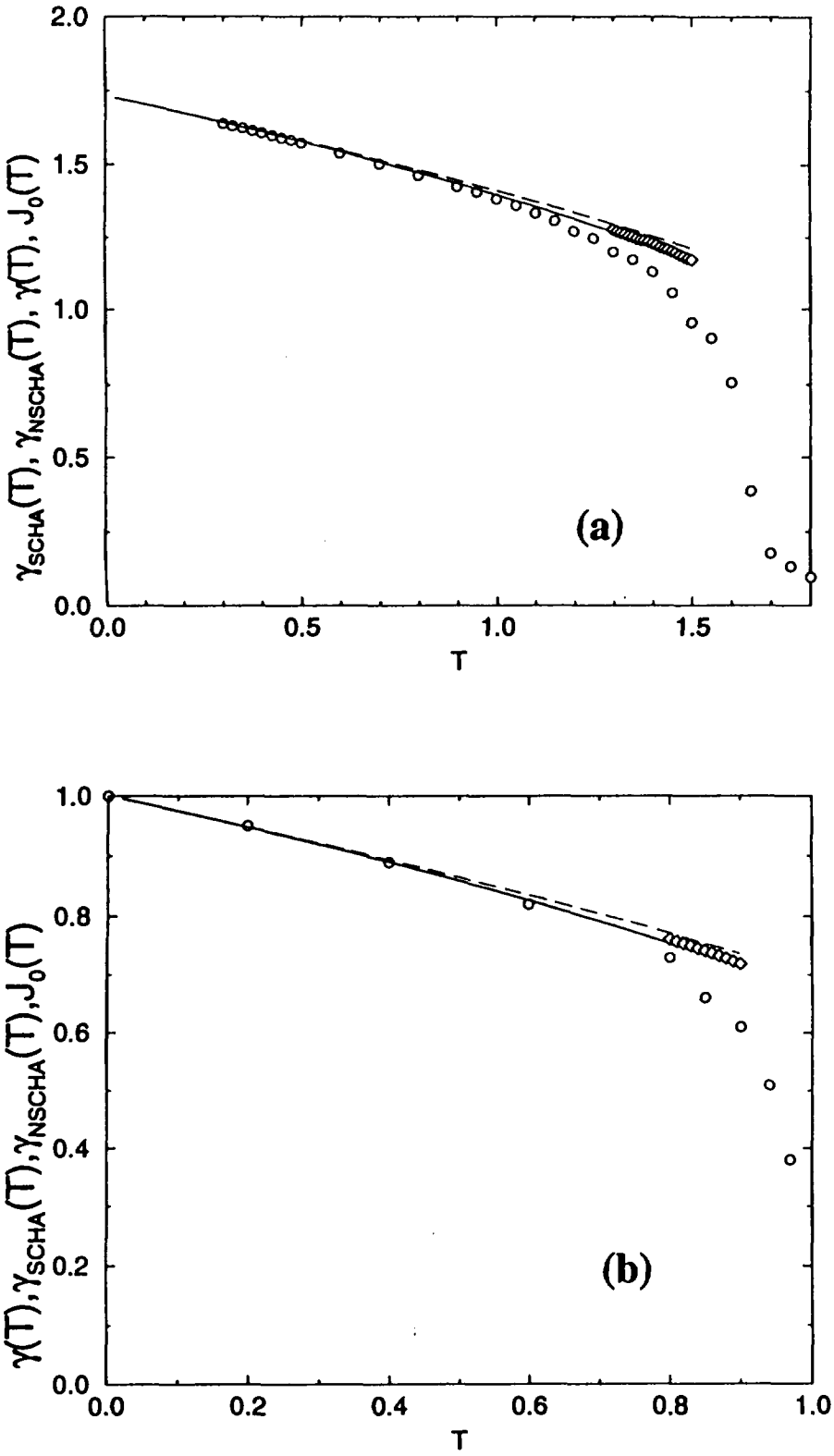

FIG. 1. Comparison of Monte Carlo and SCHA spinwave stiffnesses versus T for the ferromagnetic triangular (Fig 1.a) and square (Fig 1.b) lattices. Circles represent MC data, long-dashed lines $\gamma_{SCHA} = \tilde{J}(T)$ equ (7), solid line γ_{NSCHA} equ (26) with $\theta_i^0 = 0$. Diamonds denote MC data for the bare coupling J_0 entering the definition of the Coulomb gas temperature (equ 37).

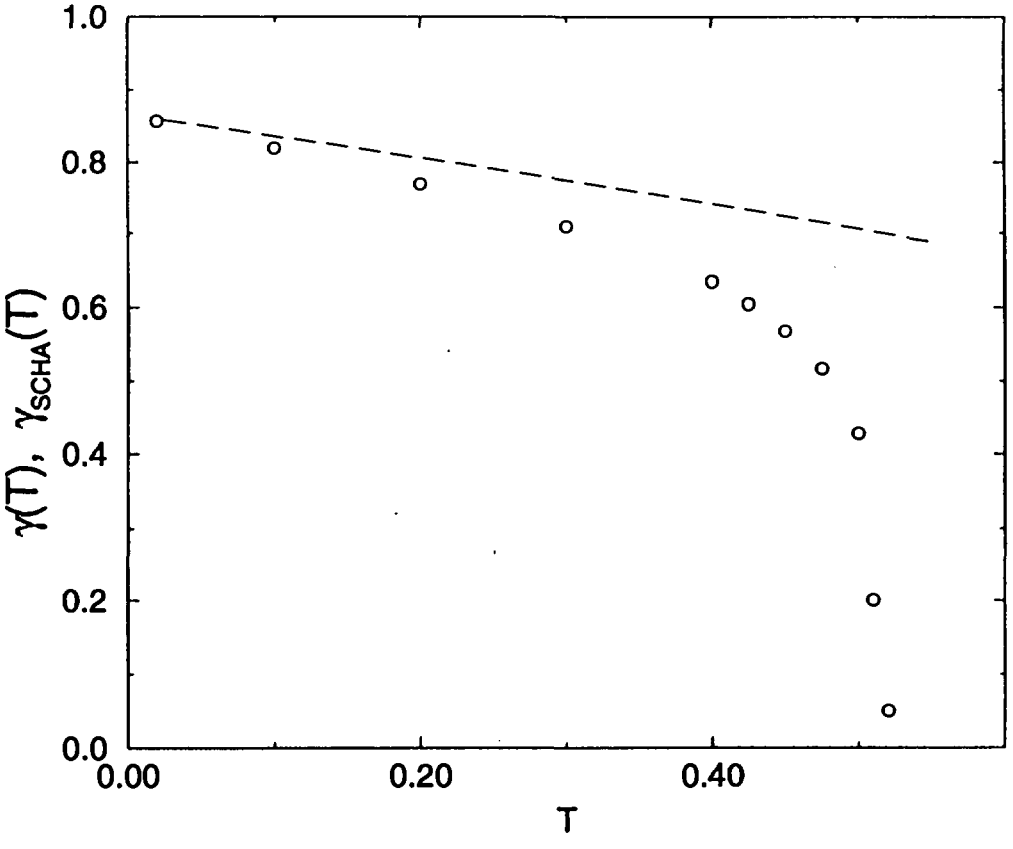

FIG. 2. Comparison of Monte Carlo and SCHA spinwave stiffnesses versus T for the fully frustrated triangular lattice. Circles represent MC data, long-dashed lines $\gamma_{SCHA} = \tilde{J}(T)$ equ (16).

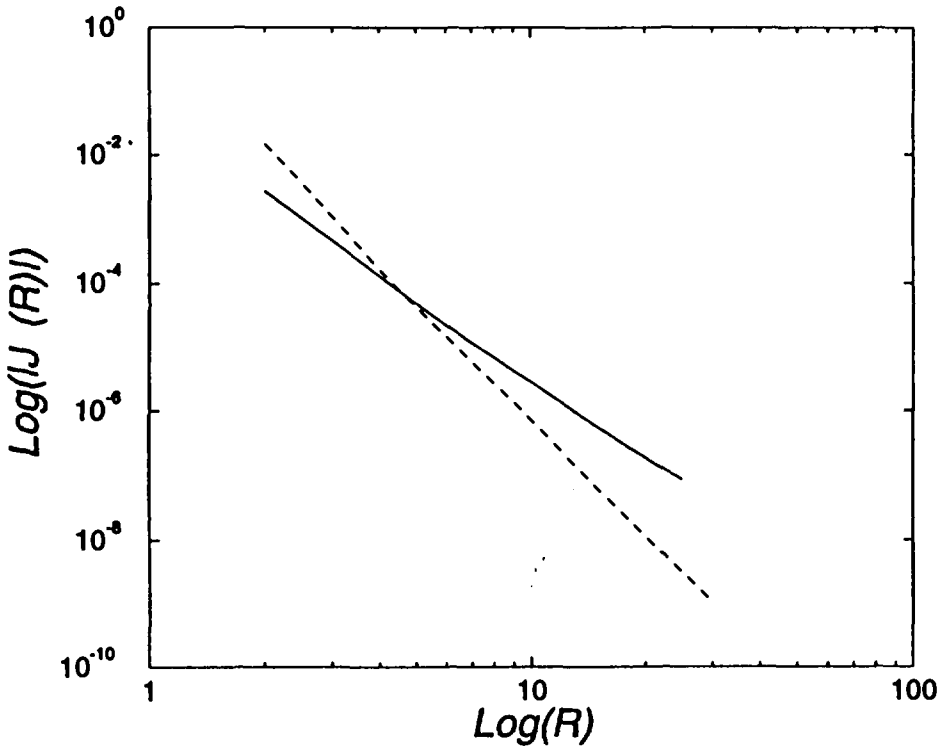

FIG. 3. $Log(|\tilde{J}(R)|)$ vs $Log(R)$ for $T = 0.4J$ for the square and triangular lattices $R = |\vec{r}_j - \vec{r}_i|$. For the SQ lattice the slope is 4 (solid line), for the TR lattice the slope is 6 (dashed line). The slope is in fact T independent (see text).

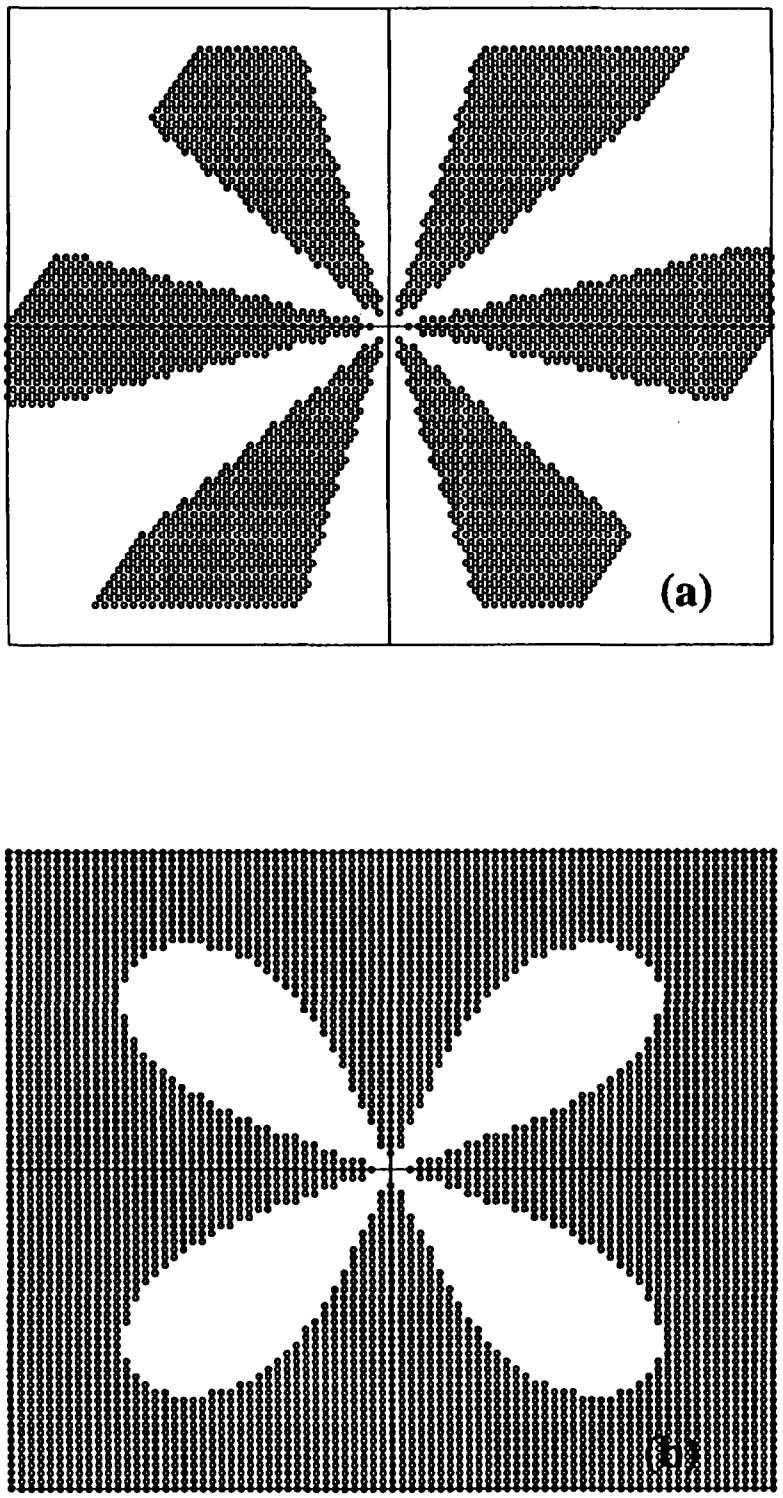

FIG. 4. The sign of $\tilde{J}_{ij}$ equ (21) at point $\vec{r}$ for the triangular lattice (Fig 4.a) and the sign of $(-1)^{x+y}\tilde{J}_{ij}$ at point $\vec{r}=(x,y)$ for the square lattice (Fig 4.b). Circles denote sites where $\tilde{J}_{ij}$ is negative.

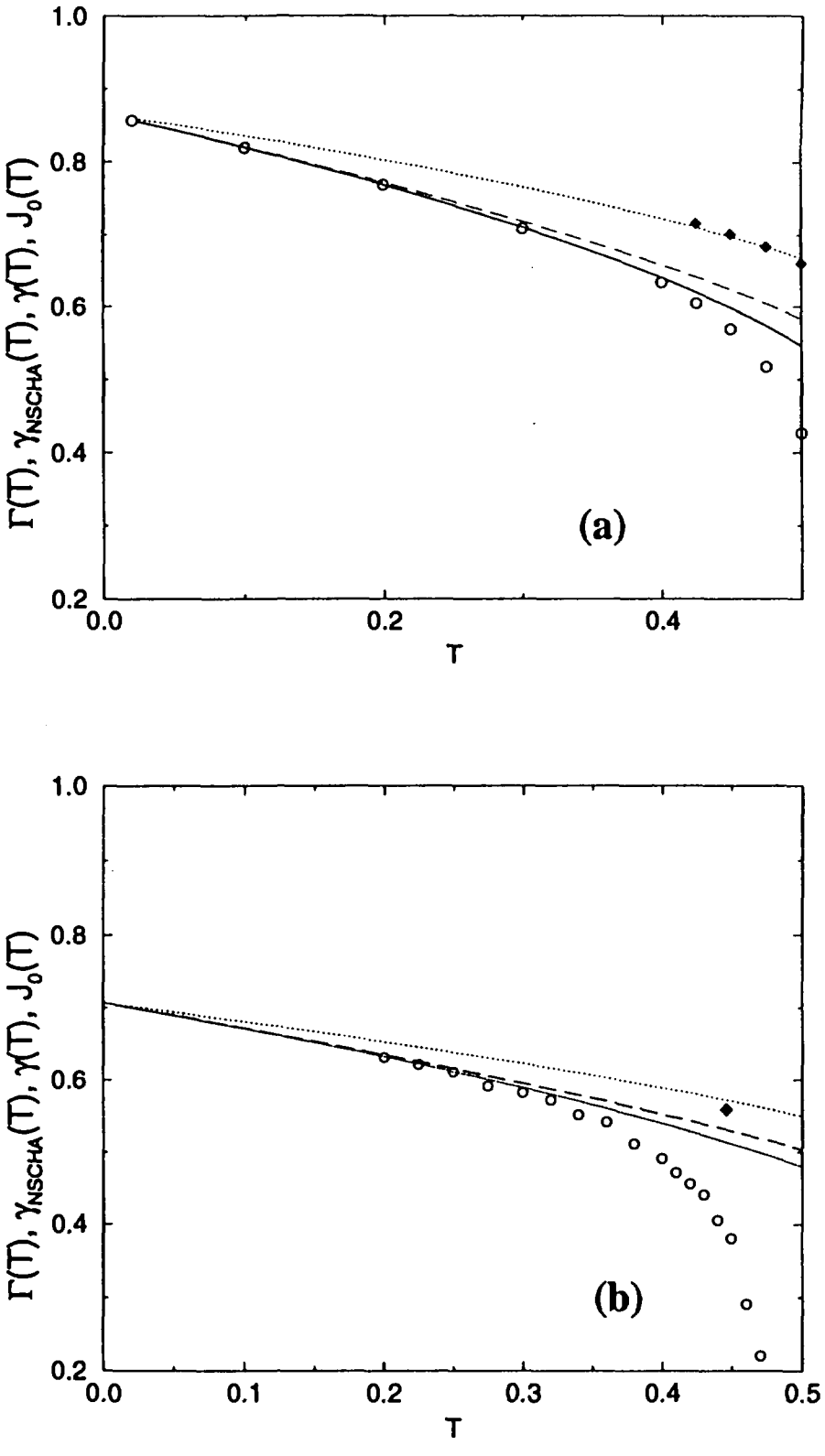

FIG. 5. Comparison of Monte Carlo and NSCHA stiffnesses versus T for the fully frustrated triangular (Fig 5.a) and square (Fig 5.b) lattices. Circles represent MC data, long-dashed lines $\Gamma(T)$ equ (25), solid line γ_{NSCHA} equ (26). Diamonds denote MC data and dotted lines the NSCHA prediction for the bare coupling J_0 entering the definition of the Coulomb gas temperature equ (38).

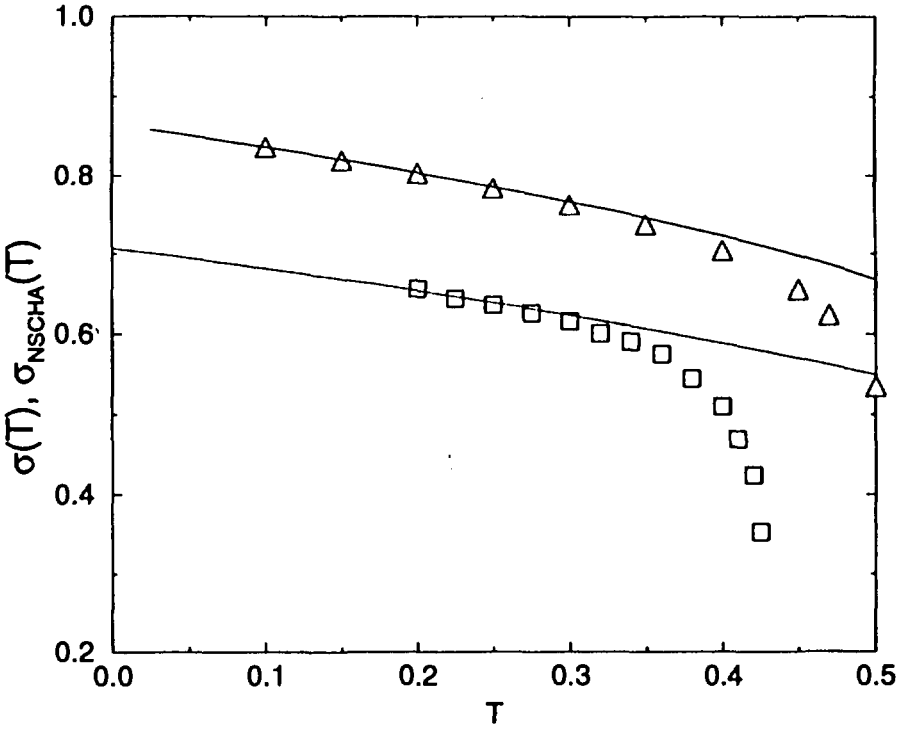

FIG. 6. Comparison of the Monte Carlo and NSCHA determined chiral order parameter σ vs T equ (31) for the TR and SQ lattices. Triangles (resp. squares) denote MC points for the triangular (resp. square) case. Solid lines are the corresponding NSCHA predictions.

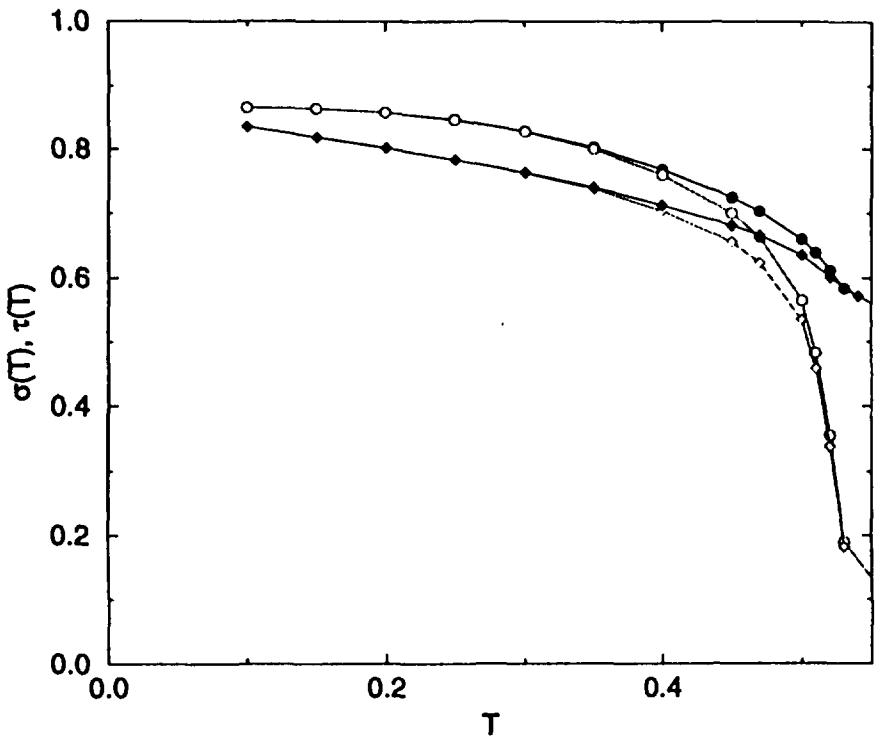

FIG. 7. MC determination of the staggered chirality $\sigma(T)$ equ (29) and of the chirality amplitude $\tau(T)$ equ (36) for the fully frustrated triangular lattice. Two definitions of σ_{kl} have been used : one is from equ (30) (open diamonds), the other is from equ (35) (open circles). They yield the same results near T_{DS}. The corresponding values of τ show as filled diamonds and filled circles respectively.

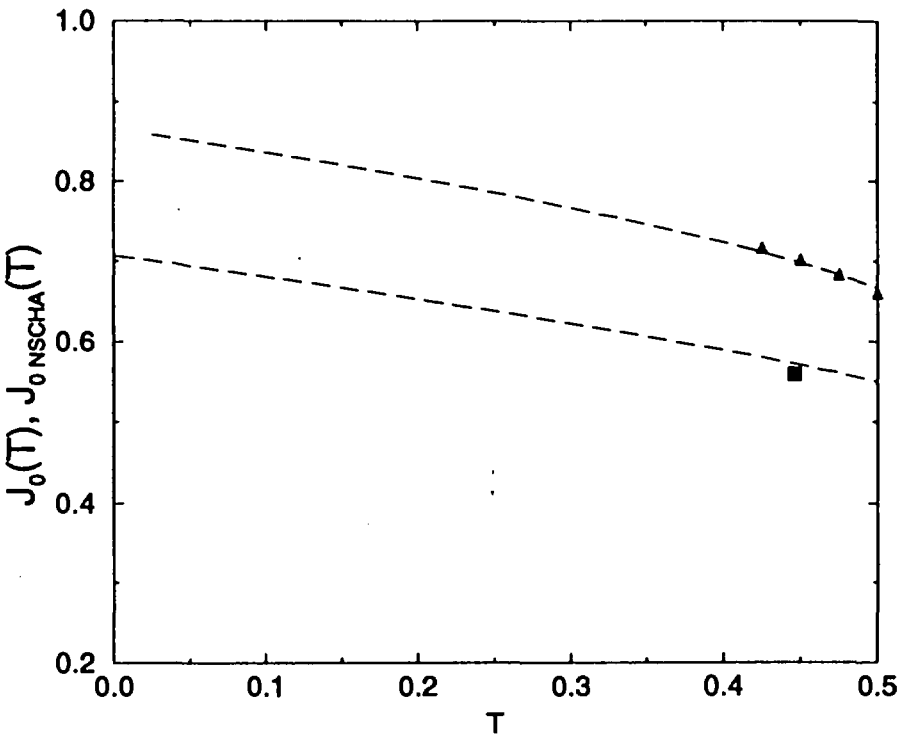

FIG. 8. Bare coupling $J_0(T)$ entering the definition of T_{CG} for the TR and for the SQ lattice near the transition. Filled triangles (resp. square) are MC data for the TR (resp. SQ) lattice. Dashed lines are the corresponding NSCHA predictions equ (38).